Paludification reduces black spruce growth rate but does not alter ecophysiological mechanisms in Canadian boreal forested peatlands

Joannie Beaulne[1,2,3*], Étienne Boucher[1,2,4], Michelle Garneau[1,2,3,4], and Gabriel Magnan[1,3]

[1] Geotop Research Center, Université du Québec à Montréal, Montréal, Québec H3C 3P8, Canada

[2] Department of Geography, Université du Québec à Montréal, Montréal, Québec H3C 3P8, Canada

[3] GRIL-UQAM, Université du Québec à Montréal, Montréal, Québec H3C 3P8, Canada

[4] Centre d'études nordiques, Université Laval, Québec, Québec G1V 0A6, Canada

* Email: joannie.beaulne@gmail.com

Abstract

Background: Paludification is widespread in the boreal biome, inducing tree growth decline in forested peatlands following the development of thick organic layers over the mineral soil. However, the ecophysiological processes involved remain poorly documented and little is known about the interactions between tree growth mechanisms and site conditions in these ecosystems. We investigated changes in stem growth and main ecophysiological processes in a black spruce forested peatland in eastern Canada by combining peat-based and tree-ring stable isotope analyses. These were conducted at three sampling sites located along a paludification gradient with different peat thicknesses.

Results: Organic layer thickening induces black spruce growth decline without altering tree ecophysiological mechanisms. A 40% increase in water use efficiency, or the ratio of carbon assimilated to water losses, was observed at the three sites from 1920 to the 1980s, but did not

translate into enhanced tree growth. A clear shift in the 1980s revealed a decline in black spruce sensitivity to climate and rising atmospheric CO_2 concentration, regardless of the organic layer thickness. Water table reconstructions revealed an important drawdown in the last few decades at the three sites, but we found no evidence of an influence of water table variations on stem growth.

Conclusions: This study shows that paludification induces black spruce growth decline without altering tree metabolism in boreal forested peatlands. This underlines that changes in water use efficiency are decoupled from changes in carbon allocation, which are constrained by site, or even tree-specific strategies to access water and nutrients from belowground. Our findings indicate that dynamic changes in edaphic conditions need to be considered in process models. Otherwise, failing to account for the degree of paludification can lead to misleading forest productivity predictions and result in considerable overestimations of aboveground carbon stocks from trees in the boreal regions.

Keywords: black spruce growth, boreal biome, climate-growth relationships, ecophysiological response, forested peatland, paludification, stable isotopes, water use efficiency

Background

Forested peatlands are widespread ecosystems in the boreal regions of the Northern Hemisphere that result from the paludification process (Korhola 1995; Crawford et al. 2003; Lavoie et al. 2005). Northern forests are particularly prone to paludification due to their cold and humid climates, particularly when combined with flat topography and fine-textured sediments (Payette 2001; Charman 2002). This process is characterised by the development of thick organic layers over the mineral sediment, favored by the establishment and expansion of *Sphagnum* mosses, which leads to humid, acid, cold, and anaerobic soil conditions (Van Cleve et al. 1983; Fenton and Bergeron 2006). This edaphic context causes forest growth decline, primarily by limiting nutrient availability

49   (Van Cleve et al. 1983; Boudreault et al. 2002; Harper et al. 2003; Simard et al. 2007), and

50   eventually results in the establishment of open and/or forested peatlands. Over the past decades,

51   many studies have focused on documenting the effects of paludification on tree biomass

52   productivity (e.g., Lecomte et al. 2006; Simard et al. 2007, 2009) and developing management

53   practices to reduce or even reverse this process in coniferous boreal forests (e.g., Heikurainen 1964;

54   Lavoie et al. 2005; Bergeron et al. 2007; Fenton et al. 2009; Lafleur et al. 2011).

55

56   While the impacts of paludification on stem growth are well understood, forest ecophysiological

57   mechanisms associated with growth decline remain unknown at the stand scale. In non-paludified

58   forests, an increase in tree intrinsic water use efficiency (i.e., the ratio of carbon assimilated to

59   water losses through evapotranspiration; Farquhar et al. 1989) associated with rising ambient CO_2

60   concentration has commonly been reported without enhancing carbon use efficiency (Manzoni et

61   al. 2018) or tree radial growth (e.g., Peñuelas et al. 2011; Silva and Horwath 2013; Lévesque et al.

62   2014). Indeed, while photosynthesis stimulation and stomatal conductance reduction control

63   changes in water use efficiency, stem growth appears to be limited by local edaphic factors, such

64   as nutrient availability (e.g., nitrogen). Paludification is thus expected to alter both water and carbon

65   use efficiency in boreal forested peatlands, given that this process induces significant changes in

66   soil conditions.

67

68   Both vegetation and hydrological dynamics in paludified settings have previously been studied

69   over millennial timescales (Ruppel et al. 2013; Le Stum-Boivin et al. 2019; Magnan et al. 2019).

70   Nonetheless, little is known about the implications of changes in ecosystem conditions on tree

71   growth mechanisms in forested peatlands. Paludification is characterized by water table rise

72   (Lavoie et al. 2005; Fenton and Bergeron 2006), and interactions over time may indeed exist

73   between water table fluctuations, tree nutrition, and stem growth responses in boreal ecosystems.

74   These interactions may influence the respective contribution of ecophysiological processes such as

75 photosynthesis and stomatal conductance, which control tree water use efficiency. Enhanced

76 knowledge of forested peatland ecophysiology may ultimately improve the modelling of the

77 response of these ecosystems to increasing CO_2 concentrations by dynamic global vegetation

78 models (DGVMs) (Pugh et al. 2016).

79

80 In this study, we aim to improve the understanding of the mechanisms that support tree radial

81 growth in black spruce (*Picea mariana* (Mill.) BSP)-forested peatlands of eastern Canada, using

82 an innovative approach that combines multi-proxy analyses. Peat-based paleoecohydrological

83 analyses were performed in parallel with stable isotope analyses in tree rings to investigate the

84 interactions between black spruce metabolism and site conditions. We hypothesise that peat

85 accumulation triggers changes in tree ecophysiological mechanisms (e.g., reduction in

86 photosynthesis rates) which result in stem growth decline. We expect this effect to be stronger in

87 the most paludified sites characterised by thicker peat deposits.

88

89 **Methods**

90 **Study area**

91 The study was conducted south of James Bay in eastern Canada, within the Clay Belt region part

92 of the black spruce-feather moss bioclimatic domain (Saucier et al. 2009; Fig. 1). This area is

93 particularly prone to paludification due to the relatively cold and humid climate, the flat

94 topography, and the dominance of poorly-drained clayey sediments left by the proglacial lakes

95 Barlow and Ojibway (Vincent and Hardy 1977; Fenton et al. 2005; Lavoie et al. 2005). Mean

96 annual temperature is 0.3°C (over the 1950-2013 period), ranging from -18.9°C in January to

97 16.3°C in July, and mean annual precipitation is 818 mm (McKenney et al. 2011). The regional fire

98 cycle is estimated to be ~400 years since 1920 (Bergeron et al. 2004), allowing the accumulation

99 of thick organic layers in forests between fire events.

100   The Casa forested peatland (49°33'06"N, 78°59'10"O; Fig. S2.1) was selected following the studies

101   of Magnan et al. (2020) and Le Stum-Boivin et al. (2019) due to its regional representativeness in

102   terms of slope, vegetation composition, and canopy openness. The organic layer thickness varies

103   between 40 cm and more than 1 m along the selected transect, and the canopy gradually opens with

104   organic layer thickening, which is typically observed in forested peatlands of the Clay Belt. The

105   aboveground vegetation is largely dominated by black spruce and ericaceous shrubs, such as

106   *Vaccinium angustifolium*, *Rhododendron groenlandicum*, *Kalmia angustifolia*, and

107   *Chamaedaphne calyculata*. The understory is dominated by *Sphagnum* communities, particularly

108   *S. angustifolium/fallax* under the tree canopy, and *S. fuscum* where the tree canopy is more open.

109
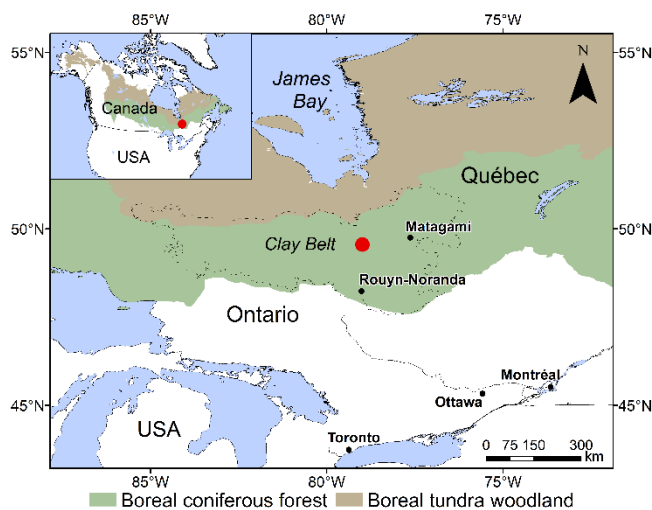
111   **Figure 1. Location of the studied Casa boreal forested peatland (red dot).**

112

113   **Sampling**

114   Three sampling sites (CAS0, CAS50, CAS100) were established along a 100 m transect following

115   an organic matter thickness gradient within the selected forested peatland (Fig. 2). At each site, one

116   peat monolith was sampled down to the mineral contact using a Box corer (Jeglum et al. 1992).

117   Sampling locations were chosen to be representative of the mean peat thickness of each site.

Relative surface altitude and peat thickness were measured at 5 m intervals along the transect using

a high precision altimeter (ZIPLEVEL PRO-2000) and an Oakfield probe. Water table depths were

measured at the same intervals a few hours after holes were dug to make sure that the water table

level had stabilized. Twenty black spruce trees were also sampled at each site within a 10 m radius

of the collected peat core. Only dominant and codominant trees with straight stems and no visible

scars were selected. Peat thickness was measured at the bottom of each sampled tree to validate the

concordance with the mean peat thickness of the site. The diameter at breast height (DBH) and the

height of selected trees were measured and cross-sections were collected at standard height (1.3 m).

The root system of one black spruce per site was excavated to verify the depth of the rooting zone,

and to identify the growth substrate (i.e., mineral or organic matter). Moreover, tree aboveground

biomass of each site was estimated by measuring the diameter at breast height (DBH) of all trees

(DBH ≥ 1 cm) within a 10×10 m plot and then using allometric equations adapted to black spruce

growth (Lambert et al. 2005; Ung et al. 2008).
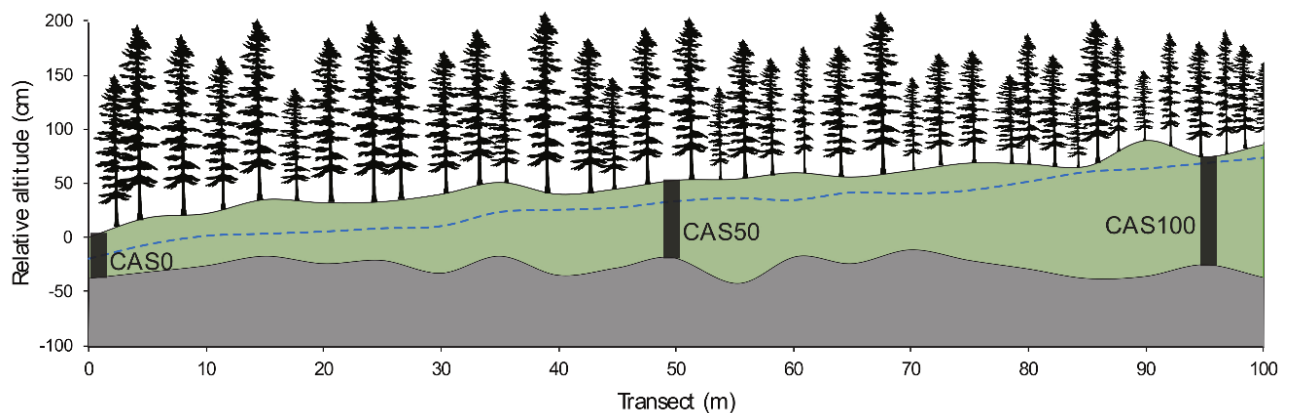
Figure 2. Schematic of the three sites along the study transect. Relative altitude of the organic

layer (green) and the mineral surface (grey) are shown. Black rectangles represent the locations of

the sampled peat cores. The dotted blue line indicates the water table level measured on the field.

Trees are not to scale but are representative of variations in canopy openness along the transect.

Peat-based paleoecohydrological reconstructions

Prior to analysis, peat cores were cut into 1 cm-thick slices. Plant macrofossils were analysed at 4 cm intervals along each peat core to reconstruct vegetation dynamics since peat initiation. Samples were prepared following the standard protocol of Mauquoy et al. (2010) and analysed in a gridded Petri dish under a stereoscopic microscope (10-40 × magnification) (SM 1.1). The relative abundances of the main peat components (e.g., *Sphagnum*, ligneous, Cyperaceae) were estimated visually and expressed as volume percentages, and vascular plant remains (e.g., seeds, needles, leaves) were counted. Macroscopic charcoal particles (>0.5 mm) were analysed at 1 cm intervals along the three peat cores to identify past local fire events.

In order to reconstruct hydrological variations, testate amoeba assemblages were also analysed at 1 cm intervals. Testate amoeba shells were extracted following the standard protocol of Booth et al. (2010) (SM 1.2). Samples were then analysed under an optical microscope (400× magnification). A minimum of 100 tests was counted per sample, except in highly humified peat samples, in which test concentration was very low. In these cases, no water table depth (WTD) was inferred, as the total count (< 20 tests) was insufficient to ensure reliable WTD reconstruction (Payne and Mitchell 2009).

Past WTDs were reconstructed using a weighted average model with tolerance down-weighting and inverse deshrinking (WA.inv.tol). The transfer function was built using the R package *rioja* (version 0.9-15.1; Juggins 2017), from a modern dataset of 272 surface samples combining non-forested open peatlands (Lamarre et al. 2013) and forested peatlands (Beaulne et al. 2018 and this study) of eastern Canada. High inferred WTD values corresponded to drier surface conditions.

Peat core chronologies

A total of 11 samples were submitted to A. E. Lalonde AMS Laboratory (University of Ottawa, Canada) for accelerator mass spectrometry radiocarbon dating (^{14}C). Plant macrofossil remains were carefully selected to date peat initiation, the last fire event, and main transitions in vegetation composition at each sampling site. The ^{14}C dates were calibrated using the IntCal13 calibration curve (Reimer et al. 2013). Additional ^{210}Pb dating was achieved for the uppermost 24-26 cm of peat cores at 1 cm intervals by alpha spectrometry (EGG Ortec 476A) at the GEOTOP Research Center (Université du Québec à Montréal, Canada). Ages were inferred by ^{210}Po activity measurement, using the constant rate of supply model (Appleby and Oldfield 1978) following HNO_3-HCl-H_2O_2 sample digestion. Further details on the ^{210}Pb dating procedure used in this study can be found in Ali et al. (2008). Age-depth models were generated using the *rbacon* package in R (version 2.3.9.1; Blaauw and Christen 2019). Ages are expressed in calendar years before present (cal yr BP; 1950 CE) and the age of the peat surface is therefore set to -67 cal yr BP (coring year: 2017 CE).

Black spruce radial growth analysis

Dried cross-sections were finely sanded (from 80 to 600 grit size) prior to ring-width measurements along two radii using CooRecorder software (version 8.1.1; Cybis Elektronik & Data AB 2016). Samples were visually cross-dated using PAST5 software (version 5.0.610; SCIEM 2019), and skeleton plots were generated using the R package *dplR* (version 1.6.9; Bunn et al. 2018). Ring-width series were converted to annual basal area increment (BAI) to compare tree aboveground productivity between the three sites, as BAI is more representative of three-dimensional stem growth than the linear ring-width measurements (Husch et al. 2003; Biondi and Qeadan 2008). Individual BAI series were produced using the R package *dplR* (version 1.6.9; Bunn et al. 2018), and yearly averages were then calculated using all trees from the same site.

188 Ring-width series were standardized using a negative exponential curve to remove cambial age

189 trends (Fritts 1976). Standardization was performed on all individual series before constructing a

190 mean standardized chronology for each site. Daily climate data (mean temperature and total

191 precipitation) from 1950 to 2013 were retrieved from the interpolated gridded climate dataset of

192 McKenney et al. (2011). Pearson correlation coefficients were calculated between standardized

193 ring-width series and monthly climate data from March to September of both the current year and

194 the year preceding ring formation. Because of time series autocorrelation, effective numbers of

195 degrees of freedom were calculated to generate adjusted p-values (Hu et al. 2017).

196

197 **Isotopic analysis of tree rings**

198 Black spruce ecophysiological response to rising ambient CO_2 concentration and climate variability

199 was evaluated from carbon ($\delta^{13}C$) and oxygen ($\delta^{18}O$) isotopic ratio analyses. These were performed

200 on five trees per site and from two wood strips per tree (i.e., a total of 30 samples). Sample

201 preparation was carried out following the protocol described in Giguère-Croteau et al. (2019) (SM

202 1.3). A five-year resolution over a 100 year period (1919-2018) was considered. Alpha-cellulose

203 was extracted, as suggested for black spruce samples (Bégin et al. 2015), following the protocol

204 used by Naulier et al. (2014).

205

206 Tree-ring $\delta^{13}C$ values vary according to discrimination against ^{13}C during photosynthesis, defined

207 as (Farquhar et al. 1982):

208

$$\Delta^{13}C = \frac{\delta^{13}C_{air} - \delta^{13}C_{tree}}{1 + (\delta^{13}C_{tree}/1000)} , \quad (1)$$

210 where $\delta^{13}C_{air}$ is the carbon isotope ratio of the atmosphere and $\delta^{13}C_{tree}$ is the isotopic value of the

211 tree ring. $\delta^{13}C_{air}$ values were taken from McCarroll and Loader (2004) for the 1919-2003 period,

212   and were linearly extrapolated for the 2004-2018 period. Because of the five-year resolution of

213    $\delta^{13}C_{tree}$ values, we averaged the $\delta^{13}C_{air}$ values over five years. According to Farquhar et al. (1989),

214    $\Delta^{13}C$ is related to leaf intercellular CO_2 concentration (c_i) and ambient CO_2 concentration (c_a)

215   according to the following equation:

216

$$\Delta^{13}C = a + (b - a)\left(\frac{c_i}{c_a}\right), \tag{2}$$

217

218   where a (4.4‰) is the fractionation occurring during CO_2 diffusion through stomata (O'Leary

219   1981) and b (27‰) is the fractionation due to carboxylation by the Rubisco enzyme (Farquhar and

220   Richards 1984). Values of c_a were obtained from the Mauna Loa Observatory

221   (esrl.noaa.gov/gmd/ccgg/). Intrinsic water use efficiency (iWUE), defined as the amount of carbon

222   assimilated per unit of water lost, can then be estimated from c_i and c_a as follows (Ehleringer et al.

223   1993):

224

$$\text{iWUE} = \left(\frac{A}{g_s}\right) = \left(\frac{c_a - c_i}{1.6}\right), \tag{3}$$

225

226   where A is the rate of CO_2 assimilation, g_s is the stomatal conductance, and the constant 1.6

227   represents the ratio of water vapor and CO_2 diffusivity in air. Equation 3 shows that the difference

228   between c_a and c_i is related to the ratio of assimilation (A) to stomatal conductance (g_s).

229

230   Since the $\delta^{18}O$ composition of tree rings is mainly controlled by leaf water composition and

231   enrichment due to transpiration of lighter oxygen isotopes, $\delta^{18}O$ values are assumed to be related

232   to the stomatal conductance and independent of photosynthetic activity (Yakir 1992; Barbour

233   2007). Therefore, by combining $\delta^{13}C$ and $\delta^{18}O$ analyses it is possible to discriminate the effects of

234   changes in photosynthetic rate (A) and stomatal behavior (g_s) on iWUE (Scheidegger et al. 2000).

Results

Paleoecohydrological reconstructions

The study sites CAS0, CAS50, and CAS100 have an organic layer thickness of 40, 75, and 100 cm respectively (Table 1). Tree-ring analyses revealed even-aged stands covering the period 1839-2018 CE at each site (see sample depth in Fig. 4 for tree age variability). Radiocarbon dating of the most recent charcoal layer indicates that the last fire event occurred between 0 and 290 cal yr BP (median age: 175-179 cal yr BP; Table S2.1). These results suggest that trees were from the first cohort that grew after the last local fire, which most likely occurred around 200-250 years ago (~1800 CE). The depth of the uppermost charcoal layer in the peat profile indicates that black spruce established in a residual organic layer of 15, 45, and 65 cm at sites CAS0, CAS50, and CAS100 respectively. The root system excavation of the three selected trees suggests that roots reached the mineral soil at CAS0 and CAS50, but were restricted to the organic layer at CAS100.

Table 1. Characteristics of the three study sites.

Site	Organic layer thickness (cm)	WTD (cm)	Mean DBH (cm)	Trees (n)	Tree biomass (kg m^{-2})	Tree density[a] (trees ha^{-1})	Mean tree height[b] (m)
CAS0	40	25	10.4	20	8.9	1200	13.8
CAS50	75	19	9.4	24	7.6	1200	11.3
CAS100	100	10	5.6	34	4.6	1000	10.4

[a] Include trees with a diameter at breast height (DBH) ≥ 9 cm

[b] Calculated from the twenty black spruce trees (dominant and co-dominant) sampled at each site.

Both hydrological conditions and vegetation composition were similar across the three sites throughout the duration of black spruce growth (Fig. S2.2, S2.3). Macrofossil analysis showed that the last fire induced a shift in vegetation composition from high dominance of woody vegetation to a black spruce-*Sphagnum*-dominated stand (Fig. S2.2). The canopy opening allowed rapid

256 *Sphagnum* moss expansion in the bryophyte layer while the black spruce post-fire cohort

257 established. Testate amoeba records indicate relatively wet conditions (high water tables) shortly

258 after the fire, followed by a gradual lowering of the water table at the three sites (Fig. 3, S2.3).

259 Inferred WTD values show very similar hydrological conditions at CAS50 and CAS100 during the

260 post-fire period (1840-2017). Both sites had stable water table depths between 15 and 20 cm before

261 water tables deepened from the 1990s, and particularly in the very recent horizons (~2010), while

262 the water table lowered more gradually at CAS0.

263
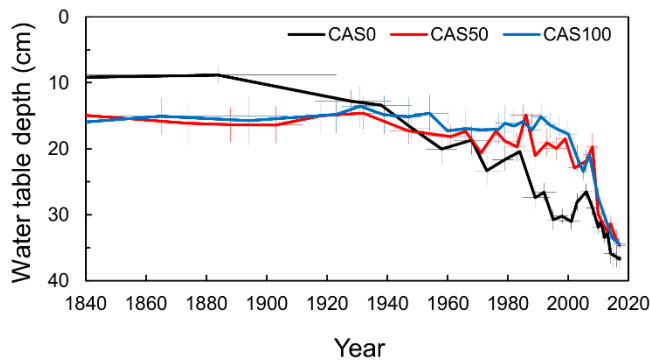
264

265 **Figure 3. WTD reconstructions for the post-fire period based on testate amoeba records.** Error

266 bars of both WTD reconstructions and age-depth modelling are shown by pale thin lines.

267

268 **Black spruce radial growth**

269 A decrease in DBH and tree height values was observed in relation with organic layer thickening

270 along the paludification gradient (Table 1). Mean DBHs of 10.4, 9.4, and 5.6 cm were calculated

271 for CAS0, CAS50, and CAS100 respectively. BAIs also indicate a decrease in stem growth with

272 increasing peat thickness (Fig. 4, S2.4). Trees from CAS0 added a greater wood surface with age,

273 especially since 1940, resulting in an increasing BAI trend (mean BAI=70 mm^2). At CAS50, tree

274 radial growth was more limited (mean BAI=51 mm^2). In contrast, trees from CAS100 maintained

275 relatively constant BAI values, resulting in decreased wood production (mean BAI=40 mm^2).

276   Estimates of tree aboveground biomass showed similar trends with values of 8.9, 7.6, and 4.6 kg/m^2

277   for sites CAS0, CAS50, and CAS100 respectively.

278
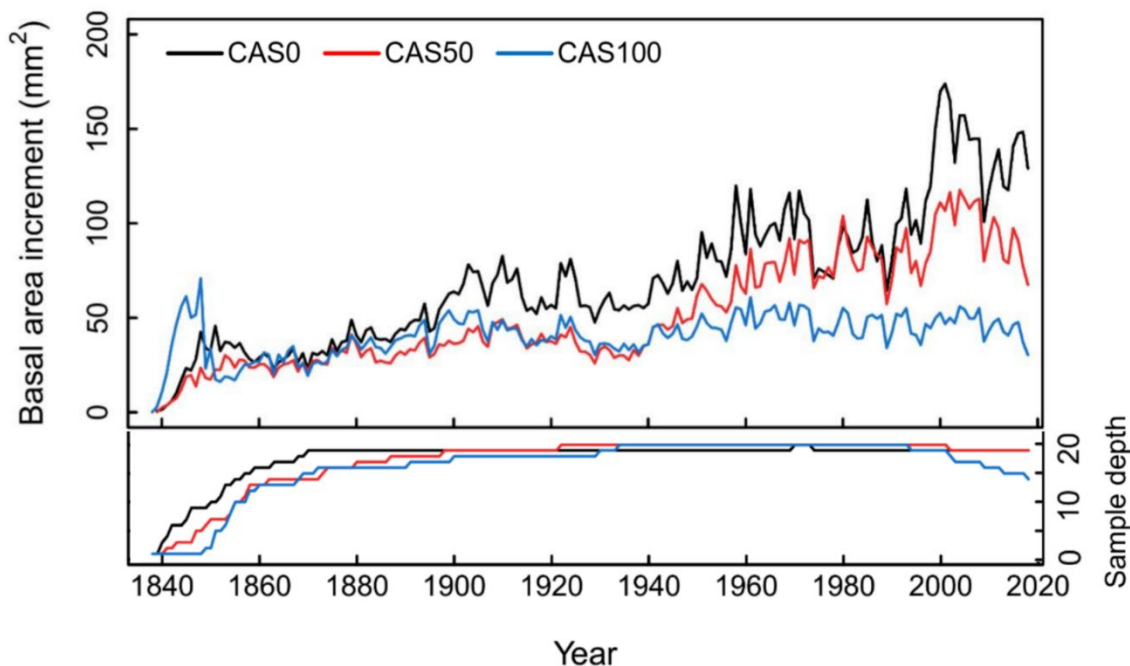
279

280   **Figure 4. Mean annual basal area increment of black spruce trees since their establishment**

281   **after the last fire event.** The decrease in sample depth at CAS100 since 2000 is explained by some

282   trees for which the latest rings were partly absent. See Fig. S2.4 for BAI distribution.

283

284   **Stem growth response to climate**

285   Pearson correlations between standardized ring-width series (Fig. S2.5) and monthly temperature

286   and precipitation data were performed separately for the 1950-1980 and 1981-2013 periods. These

287   two time periods were chosen because of the shift in black spruce ecophysiology around 1980 (see

288   next section) and the results of moving correlations with climate variables (results not shown).

289

290   Temperature's influence on tree radial growth was stronger than that of precipitation for both time

291   periods. Trees had a similar response to climate at all sites for the period 1950-1980 (Fig. 5). For

all sites, negative correlations were observed between tree stem growth and both temperature of

the previous August and April precipitation of the current year. Stem growth was also positively

correlated with September temperature of the current year. Contrastingly, stem growth barely

responded to climate during the 1981-2013 period, with much less significant and rather

heterogeneous correlations at the three sites (Fig. 5).
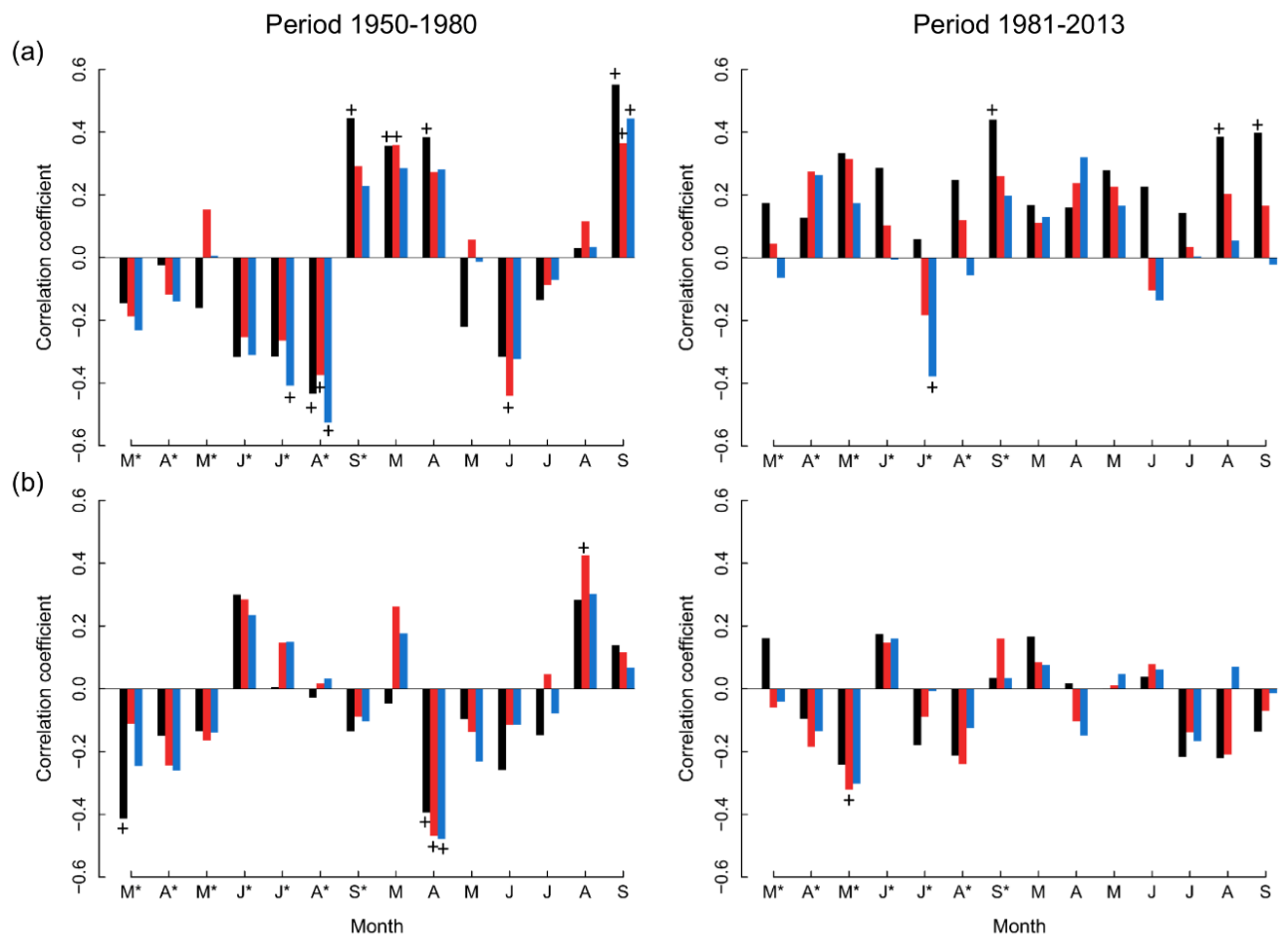
Figure 5. Pearson correlations between (a) standardized ring-width and monthly temperature, and (b) standardized ring-width and monthly precipitation for the periods 1950-1980 and 1981-2013. Correlation coefficients were calculated from March to September of the current year and the year preceding ring formation. Months from the previous year of stem

303   growth are marked with an asterisk and significant correlations ($p < 0.05$) are marked with crosses.

304   Results from CAS0, CAS50, and CAS100 are shown in black, red, and blue respectively.

305

306   Trends in $\delta^{13}C$, $\delta^{18}O$, and iWUE

307   The $\delta^{13}C$-derived ecophysiological parameters do not differ between the three sites over the 1919-

308   2000 period (Fig. 6a). Over time, black spruce trees used two different strategies in response to

309   rising c_a. A substantial increase in iWUE was first observed until the 1980s ($c_a \approx 340$ ppm), along

310   with relatively stable intercellular CO_2 concentration (c_i). During this period, iWUE increased by

311   43% at each site. A major shift in tree ecophysiology then occurred in the mid-1980s as c_i began to

312   increase considerably. In parallel, iWUE stabilized until 2018, except for at CAS0, where a new

313   increase seems to have begun around 2000.

314

315   Tree-ring cellulose $\delta^{18}O$ analyses show similar trends for the three sites across the whole record

316   (Fig. 6b). However, oxygen stable isotope ratios were systematically lower at the least paludified

317   site (CAS0), suggesting a greater depletion in heavy isotopes. For all series, tree-ring $\delta^{18}O$ values

318   increased until ~1950 and became more constant afterwards.

319

320

321
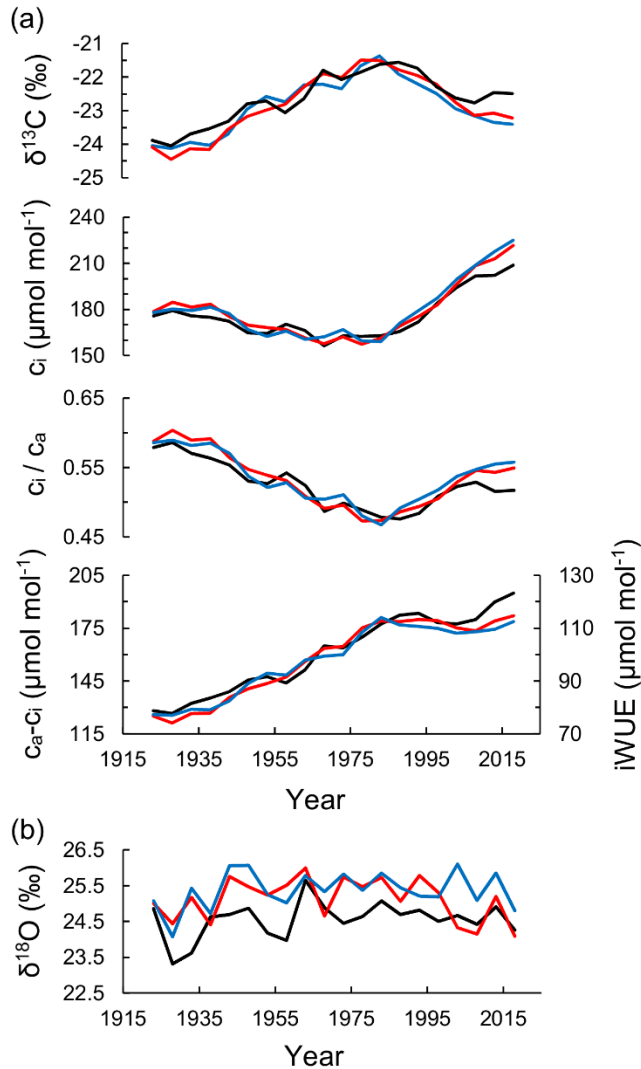
Figure 6. Black spruce ecophysiological response to rising c_α based on five-year resolution

δ^{13}C and δ^{18}O analyses for the period 1919-2018. (a) Tree-ring δ^{13}C and δ^{13}C-derived

ecophysiological parameter values (c_i, c_i/c_a, c_a- c_i, iWUE); (b) tree-ring δ^{18}O values. Results from

CAS0, CAS50, and CAS100 are shown in black, red, and blue respectively.

326

Discussion

Our study demonstrated that the degree of paludification considerably altered growth conditions

and site fertility, but did not influence intrinsic water use efficiency of black spruce trees. Indeed,

sites with the thickest organic matter accumulation were characterized by dominant trees that grew

slower, presented smaller heights and diameters (DBH), and had a lower tree density comparatively

to the least paludified site (Table 1). Surprisingly, however, $\delta^{13}C$-derived parameters are almost

identical in all sites (Fig. 6), both in terms of average iWUE levels or temporal variations,

suggesting that the ratio of photosynthesis to stomatal conductance is unaltered by the degree of

paludification. We therefore refute our research hypothesis, and cannot ascertain a clear and direct

effect of increased peat accumulation on black spruce water use efficiency and growth mechanisms.

Site fertility was recently put forward as an important parameter influencing black spruce iWUE

and its evolution with changes in c_a (Marchand et al. 2020). Based on a network of permanent

sampling plots in eastern Canada, average iWUE values were shown to be lower in the most fertile

sites (i.e., fertility being measured based on tree heights for equivalent age). Fertile sites also

experienced the most drastic iWUE increase with rising c_a, while this increase remained modest in

the least fertile sites. However, in their study, Marchand et al. (2020) examined only sites where

organic matter accumulation was inferior to 30 cm. Along our paludification gradient, peat

thickness reaches about 100 cm at CAS100 and therefore other processes linking organic matter

accumulation, water table depth, and climate need to be invoked in order to shed light on

interactions between iWUE and radial growth of black spruce in a paludified context.

Synchronous changes in iWUE over time

1920-1980s: iWUE increases (active response)

From the 1920s and until the 1980s, a ~40% iWUE increase was observed at each site, regardless

of the accumulated organic layer thickness. This significant increase, which occurred over a short

period of time, is among the highest recorded; most studies report iWUE increases of 20-30% over

the last century (e.g., Peñuelas et al. 2011; Silva and Horwath 2013; Saurer et al. 2014; Frank et al.

2015; van der Sleen et al. 2015). The increased iWUE resulted from an active response of trees

356 characterized by the maintenance of a relatively constant c_i despite rising c_a. According to

357 Scheidegger et al. (2000), when both $\delta^{13}C$ and $\delta^{18}O$ values increase, as subtly observed here until

358 the 1950s (Fig. 6), stomatal conductance most likely is the main driver of increased iWUE since it

359 is involved in the fractionation of both stable isotopes. Stomatal closure was possibly induced by

360 the combined effect of rising c_a and severe drought events that took place in the study area at the

361 beginning of the twentieth century (Girardin et al. 2004). This reduction in stomatal conductance

362 could have limited growth during the 1920-1950s period, leading to the formation of smaller and

363 narrower cells (Puchi et al. 2020; Fig. 4, S2.5). After 1950 and until the 1980s, $\delta^{13}C$ values

364 continued to increase, whereas $\delta^{18}O$ values remained relatively constant. This points to a shift in

365 acclimation strategies from a g_s-controlled iWUE to an A-controlled increase in iWUE, maintaining

366 c_i values constant.

367

368 *1980s-2010s: iWUE stabilises (passive response)*

369 In the 1980s, tree response to rising c_a suddenly became passive, as shown by the increasing c_i and

370 the relatively constant c_a-c_i (iWUE) values at all sites (Fig. 6). Likewise, a shift to a passive

371 response to increasing CO_2 concentration has previously been observed for various tree species in

372 the Canadian boreal forest (Giguère-Croteau et al. 2019; Marchand et al. 2020), in China (Wang et

373 al. 2012; Wu et al. 2015), and in Europe (Waterhouse et al. 2004; Gagen et al. 2011; Linares and

374 Camarero 2012). Three reasons might explain this shift in acclimation strategies. Firstly, this

375 finding possibly indicates reduced carbon assimilation rates (A). Indeed, in such poor growing

376 environments, the photosynthesis apparatus may saturate and nutrient limitation may downregulate

377 the capacity of trees to assimilate atmospheric carbon (Tognetti et al. 2000; Saurer et al. 2003).

378 Secondly, WTD reconstructions indicate important changes in hydrological conditions over the last

379 30 years (Fig. 3) that might have altered black spruce iWUE. The recent water table drawdown

380 could have generated stressful growth conditions since black spruce develops adventitious roots

that are generally confined to the upper 20-30 cm of the organic layer (Lieffers and Rothwell 1987; Viereck and Johnson 1990). However, such a drop in WTD would have most certainly been accompanied by a reduction in stomatal conductance, which was not observed here. Moreover, it remains unclear whether the apparent drying trend reflects increasingly drier site conditions or simply an enhanced vertical *Sphagnum* mosses growth that disconnects the peat surface from the water table. Increasingly warmer conditions since the 1990s (Fig. S2.6) could have triggered this rapid peat accumulation (Magnan et al. 2018; van Bellen et al. 2018; Primeau and Garneau, under review; Robitaille et al. submitted). The rapid accumulation of organic matter may have exceeded the capacity of adventitious roots to develop higher in the soil profile, compromising the access to oxygen. Lastly, considering that black spruce trees were approximately 180 years old in the 1980s, we cannot rule out the stand age as another potential cause for the reduction in iWUE (Irvine et al. 2004; Kutsch et al. 2009; Marchand et al. 2020).

Stem growth is decoupled from iWUE variations

Our results indicate that lower radial growth rates are found with increasing peat accumulation (Fig. 4). This effect was also reported in the black spruce feather moss domain of the James Bay and Abitibi lowlands of eastern Canada (Harper et al. 2003; Fenton et al. 2005; Lecomte et al. 2006; Simard et al. 2007). Low stem growth rates have mostly been attributed to the decrease in nutrient availability induced by peat accumulation (Van Cleve and Viereck 1981; Prescott et al. 2000; Simard et al. 2007). Nitrogen concentration is particularly low in peat deposits and consequently, the effect of limited nitrogen availability on boreal forest growth (Macdonald and Lieffers 1990; Tamm 1991; Vitousek and Howarth 1991; Maynard et al. 2014) is certainly exacerbated by paludification. The thickness of the post-fire residual organic layer in which black spruce trees established is thereby critical in determining tree nutrient uptake and aboveground biomass production. It is well established that black spruce roots can penetrate to a depth of about 60 cm,

although they are generally limited to the upper 20-30 cm (Lieffers and Rothwell 1987; Viereck and Johnson 1990). Trees from CAS0 and CAS50 both established in a less than 50 cm-thick organic horizon, and roots could therefore easily reach the mineral soil, resulting in higher radial growth rates at these sites. On the other hand, tree roots were unable reach the mineral soil layer at CAS100 as black spruce trees established in a 67 cm-deep organic layer.

These findings imply that processes controlling carbon use and allocation to radial tree growth are decoupled from those that control iWUE. This is in agreement with studies suggesting that iWUE increases do not directly translate into enhanced radial growth (e.g., Peñuelas et al. 2011; Lévesque et al. 2014; van der Sleen et al. 2015; Giguère-Croteau et al. 2019). Based on a comparison of tree ring widths and eddy-covariance flux towers in boreal Canada, Pappas et al. (2020) showed that aboveground biomass, and most particularly radial stem growth, represents only a minor fraction (~9%) of the total gross ecosystem production (GEP). Rocha et al. (2006) also found that stem growth, as estimated from tree ring widths, was not correlated to eddy-covariance-derived GEP in the boreal forest of central Manitoba. These findings point into the same direction: gas exchanges at the vegetation-atmosphere interface are controlled at the leaf level, but the allocation of newly formed photosynthates to either above- or below-ground compartments may depend on local growing conditions and site-specific growth strategies. Our study must therefore be seen as an extreme case where paludification induced locally-important edaphic changes that resulted in large differences in site fertility. Prioritization of belowground growth was more important in the most paludified (least fertile) sites, neglecting carbon allocation to aboveground compartments. This allocation strategy could reinforce tree anchoring (Nicoll et al. 2006) and enhance nutrient uptake (Vicca et al. 2012; Fernández-Martínez et al. 2014), but further research is needed to shed light on the processes driving allocation changes in black spruce trees.

431　The proportionality of the A/g_s ratio needs to be preserved between sites in order to maintain

432　comparable iWUE values across the paludification gradient (both in terms of mean and variability).

433　This implies that if A is higher in the least paludified site (e.g., CAS0) and lower in the most

434　paludified site (e.g., CAS100), then g_s will adjust in such a way to maintain nearly identical A/g_s

435　ratio, and consequently, iWUE values. Actually, we suspect that this proportional adjustment in the

436　A/g_s ratio might be an important process driving interactions between iWUE and growth rates in a

437　paludified context. As a supporting evidence for this, we found that black spruce tree ring cellulose

438　from the least paludified site (CAS0) was significantly more depleted in ^{18}O compared to that of

439　other sites (Fig. 6b). Unsurprisingly, CAS0 is also the site where radial growth rates are the highest.

440　Increased evapotranspiration rates are probably required to sustain enhanced carbon assimilation

441　and growth rates, forcing g_s to level up and proportionally adjust to increases in A (matching the

442　ratio of other sites). Consequently, higher evapotranspiration rates cause black spruce to pump more

443　^{18}O-depleted water from soil depths (Evaristo et al. 2017), which in turns decreases average δ^{18}O

444　of tree ring cellulose.

445

446　**A shift in tree response to climate in the 1980s**

447　Difference in peat thickness along the paludification gradient did not have a noticeable influence on

448　tree response to climate. Before the 1980s, tree growth from all sites showed negative correlations

449　with previous summer temperatures (Fig. 5). These climate-growth relationships have previously

450　been reported for the Canadian boreal forest (e.g., Drobyshev et al. 2010; Walker and Johnstone

451　2014; Girardin et al. 2016; Gennaretti et al. 2017). High summer temperatures in the previous

452　growing season can restrict carbon reserve accumulation, which shapes early wood development

453　the next growing season (Fritts 1976; Skomarkova et al. 2006; Campioli et al. 2011). Black spruce

454　growth also responded positively to September temperature of the current year and negatively to

455 April precipitation of the current year, which suggests that stem growth benefits from a longer

456 growing season.

457

458 After the 1980s, trees however became much less sensitive to temperature and precipitation

459 (Fig. 5). This could possibly represent a collateral effect of paludification. Interestingly, the shift

460 indicating a clear decline in black spruce sensitivity to climate is synchronous with the decline in

461 iWUE. The reduced sensitivity of trees to temperature since the mid-twentieth century has been

462 reported in previous tree ring studies of northern latitudinal forests, and has been referred to as the

463 "divergence problem" (e.g., Briffa et al. 2004; D'Arrigo et al. 2008; Esper and Frank 2009;

464 Schneider et al. 2014). This "divergence" phenomenon could potentially be caused by thresholded

465 responses or stresses induced by changes in growth conditions (D'Arrigo et al. 2008). The

466 important WTD deepening over the last decades (Fig. 3) might have contributed, along with stand

467 age (Szeicz and MacDonald 1994; Konter et al. 2016), to the decline in tree sensitivity to climate

468 (at the stem level) in our sites.

469

470 Overall, this study represents a first attempt to unravel the numerous and complex entanglements

471 between paludification dynamics and forest ecophysiology in the boreal forest of eastern Canada.

472 Based on our results, we conclude that taking into account factors reflecting site edaphic conditions

473 is essential to better describe and predict forest response to environmental variability, especially in

474 nutrient-limited ecosystems (Ainsworth and Rogers 2007; Kirschbaum 2011; Lévesque et al. 2016;

475 Guerrieri et al. 2019). Our findings warrant further studies of vegetation/forest dynamics models

476 and their application to forested peatlands, as those models are often biased towards converting

477 increases in iWUE into increases in stem growth. For example, a successful modelling of the c_i/c_a

478 ratio based on the least-cost optimality principle (Lavergne et al. 2020) would predict comparable

479 iWUE trends, regardless of the degree of paludification and with correct implications for carbon

480 and water cycle interactions at the leaf level. However, failing to account for paludification-related

481   carbon allocation strategies would result in the overestimation of aboveground biomass production

482   in sites where peat accumulation is rapid. Peatlands are one the largest natural terrestrial ecosystems

483   for carbon sequestration, and forested peatlands represent a major component of these ecosystems

484   in boreal regions (Thompson et al. 2016; Webster et al. 2018). Therefore, additional research on

485   carbon allocation strategies are of utmost importance to understanding the carbon sink capacity of

486   black-spruce-dominated boreal ecosystems.

487

Conclusions

489   In this study, we used an innovative approach to evaluate black spruce radial growth in sites

490   undergoing paludification by combining paleoecohydrological, dendrochronological, and

491   geochemical analyses. We provide the first multi-proxy tree-ring chronologies showing how radial

492   tree growth and main metabolic processes change along a paludification gradient.

493

494   Contrary to our expectations, results show that the degree of paludification does not alter black

495   spruce metabolism in boreal forested peatlands. The accumulation of thick organic layers does

496   induce stem growth decline, but this tree response to paludification is not reflected in black spruce

497   ecophysiological mechanisms. The increasing iWUE trends observed could suggest increasing

498   carbon assimilation and radial growth rates at the three sites. However, radial growth of black

499   spruce trees clearly declined with organic layer thickness, resulting in different tree aboveground

500   biomass between the study sites. This underlines that changes in iWUE are not necessarily related

501   to changes in carbon use efficiency because of site conditions (Manzoni et al. 2018). Consequently,

502   dynamic changes in edaphic conditions need to be considered in process models (Guiot et al. 2014).

503   Otherwise, based on tree ecophysiological parameters alone, comparable growth between the three

504   study sites would have been assumed. Our results thus suggest that failing to account for degree of

505   paludification in interpreting tree growth mechanisms can lead to misleading forest productivity

predictions in the boreal biome. This could furthermore result in a considerable overestimation of carbon stocks from trees in the boreal regions where paludified forests and forested peatlands are widespread.

Declarations

Acknowledgements

We are grateful to Pierre Grondin (MFFP) for his precious contribution to this project. Thanks to Nolann Chaumont and Camille Lepage for their help with field and laboratory work. Special thanks to Nicole Sanderson for her help with ^{210}Pb dating. We also thank *Les Tourbeux.ses* for their help and useful advice.

Authors' contributions

All authors designed the research and conducted the fieldwork. J.B. performed the research and É.B., M.G. and G.M. helped analyzing the data. J.B. wrote the first draft of the manuscript and all authors contributed critically to subsequent drafts and gave final approval for publication.

Funding

Scholarships to J.B. were provided by the Natural Sciences and Engineering Research Council of Canada (NSERC-CGS M) and the Fonds de recherche du Québec – Nature et technologies (FRQNT). Fieldwork and analyses were funded by the Natural Sciences and Engineering Research Council of Canada through discovery grants to M.G. (NSERC #250287) and É.B. (RGPIN-2016-05244).

530   **Availability of data and materials**

531   Data will be archived on the Tree-Ring network of Qc-Lab database: http://dendro-qc-lab.ca

532

533   **Competing interests**

534   The authors declare no competing interests.

535

536   **Ethics approval and consent to participate**

537   Not applicable.

538

539   **Consent for publication**

540   Not applicable.

541

References

543   Ainsworth EA, Rogers A (2007) The response of photosynthesis and stomatal conductance to rising

544   [CO2]: mechanisms and environmental interactions. Plant Cell Environ 30:258-270.

545   Ali AA, Ghaleb B, Garneau M, Asnong H, Loisel J (2008) Recent peat accumulation rates in

546   minerotrophic peatlands of the Bay James region, Eastern Canada, inferred by ^{210}Pb and ^{137}Cs

547   radiometric techniques. Appl Radiat Isot 66:1350-1358.

548   Appleby PG, Oldfield F (1978) The calculation of ^{210}Pb dates assuming a constant rate of supply

549   of unsupported ^{210}Pb to the sediment. Catena 5:1-8.

550   Barbour MM (2007) Stable oxygen isotope composition of plant tissue: A review. Funct Plant Biol

551   34:83-94.

552   Beaulne J, Magnan G, Garneau M (2018) Evaluating the potential of testate amoebae as indicators

553   of hydrological conditions in boreal forested peatlands. Ecol Indic 91:386-394.

554   Bégin C, Gingras M, Savard MM, Marion J, Nicault A, Bégin Y (2015) Assessing tree-ring carbon

555   and oxygen stable isotopes for climate reconstruction in the Canadian northeastern boreal forest.

556   Palaeogeogr Palaeoclimatol Palaeoecol 423:91-101.

557   Bergeron Y, Drapeau P, Gauthier S, Lecomte N (2007) Using knowledge of natural disturbances

558   to support sustainable forest management in the northern Clay Belt. For Chron 83:326-337.

559   Bergeron Y, Gauthier S, Flannigan MD, Kafka V (2004) Fire regimes at the transition between

560   mixedwood and coniferous boreal forest in northwestern Quebec. Ecology 85:1916-1932.

561   Biondi F, Qeadan F (2008) A theory-driven approach to tree-ring standardization: defining the

562   biological trend from expected basal area increment. Tree Ring Res 64:81-96.

563   Blaauw M, Christen JA (2019) rbacon: Age-Depth Modelling using Bayesian Statistics. R package

564   version 2.3.9.1. https://CRAN.R-project.org/package=rbacon

565   Booth RK, Lamentowicz M, Charman DJ (2010) Preparation and analysis of testate amoebae in

566   peatland palaeoenvironmental studies. Mires Peat 7:1-7.

567   Boudreault C, Bergeron Y, Gauthier S, Drapeau P (2002) Bryophyte and lichen communities in

568   mature to old-growth stands in eastern boreal forests of Canada. Can J For Res 32:1080-1093.

569   Briffa KR, Osborn TJ, Schweingruber FH (2004) Large-scale temperature inferences from tree

570   rings: a review. Glob Planet Change 40:11-26.

571   Bunn A, Korpela M, Biondi F, Campelo F, Mérian P, Qeadan F, … Wernicke J (2018) dplR:

572   Dendrochronology Program Library in R. R package version 1.6.9. https://CRAN.R-

573   project.org/package=dplR

574 Campioli M, Gielen B, Göckede M, Papale D, Bouriaud O, Granier A (2011) Temporal variability

575 of the NPP-GPP ratio at seasonal and interannual time scales in a temperate beech forest.

576 Biogeosciences 8:2481-2492.

577 Charman D (2002) Peatlands and environmental change. John Wiley & Sons Ltd, Chichester.

578 Crawford RMM, Jeffree CE, Rees WG (2003) Paludification and forest retreat in northern oceanic

579 environments. Ann Bot 91:213-226.

580 Cybis Elektronik & Data AB (2016) CooRecorder version 8.1.1. Cybis, Saltsjöbaden.

581 D'Arrigo R, Wilson R, Liepert B, Cherubini P (2008) On the 'Divergence Problem' in Northern

582 Forests: A review of the tree-ring evidence and possible causes. Glob Planet Change 60:289-305.

583 Drobyshev Y, Simard M, Bergeron Y, Hofgaard A (2010) Does soil organic layer thickness affect

584 climate–growth relationships in the black spruce boreal ecosystem? Ecosystems 13:556-574.

585 Ehleringer JR, Hall AE, Farquhar GD (1993) Stable isotopes and plant carbon–water relations.

586 Academic Press, New York.

587 Esper J, Frank D (2009) Divergence pitfalls in tree-ring research. Clim Change 94:261-266.

588 Evaristo J, McDonnell JJ, Clemens J (2017) Plant source water apportionment using stable

589 isotopes: A comparison of simple linear, two-compartment mixing model approaches. Hydrol

590 Process 31:3750-3758.

591 Farquhar GD, Ehleringer JR, Hubick KT (1989) Carbon isotope discrimination and photosynthesis.

592 Annu Rev Plant Physiol 40:503-537.

593 Farquhar GD, O'Leary MH, Berry JA (1982) On the relationship between carbon isotope

594 discrimination and the intercellular carbon dioxide concentration in leaves. Aust J Plant Physiol

595 9:121-137.

596 Farquhar GD, Richards RA (1984) Isotopic composition of plant carbon correlates with water-use

597 efficiency of wheat genotypes. Aust J Plant Physiol 11:539-552.

598 Fenton N, Bergeron Y (2006) Facilitative succession in a boreal bryophyte community driven by

599 changes in available moisture and light. J Veg Sci 17:65-76.

600 Fenton N, Lecomte N, Légaré S, Bergeron Y (2005) Paludification in black spruce (*Picea mariana*)

601 forests of eastern Canada: Potential factors and management implications. For Ecol Manag

602 213:151-159.

603 Fenton NJ, Simard M, Bergeron Y (2009) Emulating natural disturbances: the role of silviculture

604 in creating even-aged and complex structures in the black spruce boreal forest of eastern North

605 America. J For Res 14:258-267.

606 Fernández-Martínez M, Vicca S, Janssens IA, Sardans J, Luyssaert S, Campioli M, … Peñuelas, J

607 (2014) Nutrient availability as the key regulator of global forest carbon balance. Nat Clim Change

608 4:471-476.

609 Frank DC, Poulter B, Saurer M, Esper J, Huntingford C, Helle G, … Weigl M (2015) Water-use

610 efficiency and transpiration across European forests during the Anthropocene. Nat Clim Change

611 5:579-583.

612 Fritts HC (1976) Tree rings and climate. Academic Press, New York.

613 Gagen M, Finsinger W, Wagner-Cremer F, Mccarroll D, Loader NJ, Robertson I, … Kirchhefer A

614 (2011) Evidence of changing intrinsic water-use efficiency under rising atmospheric CO_2

615 concentrations in Boreal Fennoscandia from subfossil leaves and tree ring $\delta^{13}C$ ratios. Glob Change

616 Biol 17:1064-1072.

617   Gennaretti F, Gea-Izquierdo G, Boucher É, Berninger F, Arseneault D, Guiot J (2017)

618   Ecophysiological modeling of photosynthesis and carbon allocation to the tree stem in the boreal

619   forest. Biogeosciences 14:4851–4866.

620   Giguère-Croteau C, Boucher É, Bergeron Y, Girardin MP, Drobyshev I, Silva LCR, … Garneau

621   M (2019) North America's oldest boreal trees are more efficient water users due to increased

622   [CO2], but do not grow faster. Proc Natl Acad Sci USA 116:2749-2754.

623   Girardin MP, Bouriaud O, Hogg EH, Kurz W, Zimmermann NE, Metsaranta JM, … Bhatti J (2016)

624   No growth stimulation of Canada's boreal forest under half-century of combined warming and CO_2

625   fertilization. Proc Natl Acad Sci USA 113:E8406-E8414.

626   Girardin M-P, Tardif J, Flannigan MD, Bergeron Y (2004) Multicentury reconstruction of the

627   Canadian Drought Code from eastern Canada and its relationship with paleoclimatic indices of

628   atmospheric circulation. Clim Dyn 23:99-115.

629   Guerrieria R, Belmecheri S, Ollinger SV, Asbjornsen H, Jennings K, Xiao J, … Richardson AD

630   (2019) Disentangling the role of photosynthesis and stomatal conductance on rising forest water-

631   use efficiency. Proc Natl Acad Sci USA 116:16909-16914.

632   Guiot J, Boucher É, Gea-Izquierdo G (2014) Process models and model-data fusion in

633   dendroecology. Front Ecol Evol 2:1-12.

634   Harper K, Boudreault C, DeGrandpré L, Drapeau P, Gauthier S, Bergeron Y (2003) Structure,

635   composition, and diversity of old-growth black spruce forest of the Clay Belt region in Quebec and

636   Ontario. Environ Rev 11:S79-S98.

637   Heikurainen L (1964) Improvement of Forest Growth on Poorly Drained Peat Soils. Int Rev For

638   Res 1:39-113.

639   Hu J, Emile-Geay J, Pardin J (2017) Correlation-based interpretations of paleoclimate data – where

640   statistics meet past climates. Earth Planet Sci Lett 459:362-371.

641   Husch B, Beers TW, Kershaw Jr JA (2003) Forest Mensuration (4th ed.). John Wiley & Sons, New

642   York.

643   Irvine J, Law BE, Kurpius MR, Anthoni PM, Moore D, Schwarz PA (2004) Age-related changes

644   in ecosystem structure and function and effects on water and carbon exchange in ponderosa pine.

645   Tree Physiol 24:753-763.

646   Jeglum JK, Rothwell RL, Berry GJ, Smith GKM (1992) A Peat Sampler for Rapid Survey.

647   Frontline, Technical Note 13 921-932. Canadian Forestry Service, Sault-Sainte-Marie.

648   Juggins S (2017) rioja: Analysis of Quaternary Science Data. R package version 0.9-15.1.

649   http://cran.r-project.org/package=rioja.

650   Kirschbaum MUF (2011) Does enhanced photosynthesis enhance growth? Lessons learned from

651   CO_2 enrichment studies. Plant Physiol 155:117-124.

652   Konter O, Büntgen U, Carrer M, Timonen M, Esper J (2016) Climate signal age effects in boreal

653   tree-rings: Lessons to be learned for paleoclimatic reconstructions. Quat Sci Rev 142:164-172.

654   Korhola A (1995) Holocene climatic variations in southern Finland reconstructed from peat-

655   initiation data. Holocene 5:43-58.

656   Kutsch WL, Wirth C, Kattge J, Nöllert S, Herbst M, Kappen L (2009) Ecophysiological

657   characteristics of mature trees and stands – consequences for old-growth forest productivity. In C

658   Wirth, G Gleixner, M Heimann (Eds.) Old-Growth Forests – Function, Fate and Value. Springer-

659   Verlag, Heidelberg.

660   Lafleur B, Paré D, Fenton NJ, Bergeron Y (2011) Growth of planted black spruce seedlings

661   following mechanical site preparation in boreal forested peatlands with variable organic layer

662   thickness: 5-year results. Ann For Sci 68:1291-1302.

663   Lamarre A, Magnan G, Garneau M, Boucher É (2013) A testate amoeba-based transfer function

664   for paleohydrological reconstruction from boreal and subarctic peatlands in northeastern Canada.

665   Quat Int 306:88-96.

666   Lambert MC, Ung CH, Raulier F (2005) Canadian national tree aboveground biomass

667   equations. *Can J For Res* 35:1996–2018.

668   Lavergne A, Voelker S, Csank A, Graven H, de Boer HJ, Daux V, … Prentice IC (2020) Historical

669   changes in the stomatal limitation of photosynthesis: empirical support for an optimality principle.

670   New Phytol 225:2484-2497.

671   Lavoie M, Paré D, Fenton N, Groot A, Taylor K (2005) Paludification and management of forested

672   peatlands in Canada: a literature review. Environ Rev 13 :21-50.

673   Le Stum-Boivin É, Magnan G, Garneau M, Fenton NJ, Grondin P, Bergeron Y (2019)

674   Spatiotemporal evolution of paludification associated with autogenic and allogenic factors in the

675   black spruce–moss boreal forest of Québec, Canada. Quat Res 91:650-664.

676   Lecomte N, Simard M, Bergeron Y (2006) Effects of fire severity and initial tree composition on

677   stand structural development in the coniferous boreal forest of northwestern Québec, Canada.

678   Écoscience 13:152-163.

679   Lévesque M, Siegwolf R, Saurer M, Eilmann B, Rigling A (2014) Increased water-use efficiency

680   does not lead to enhanced tree growth under xeric and mesic conditions. New Phytol 203:94-109.

681   Lévesque M, Walthert L, Weber P (2016) Soil nutrients influence growth response of temperate

682   tree species to drought. J Ecol 104:377-387.

683   Lieffers VJ, Rothwell RL (1987) Rooting of peatland black spruce and tamarack in relation to depth

684   of water table. Can J Bot 65:817-821.

685   Linares JC, Camarero JJ (2012) From pattern to process: linking intrinsic water-use efficiency to

686   drought-induced forest decline. Glob Change Biol 18:1000-1015.

687   MacDonald SE, Lieffers VJ (1990) Photosynthesis, water relations, and foliar nitrogen of *Picea*

688   *mariana* and *Larix laricina* from drained and undrained peatlands. Can J For Res 20:995-1000.

689   Magnan G, Garneau M, Le Stum-Boivin É, Grondin P, Bergeron Y (2020) Long-term carbon

690   sequestration in boreal forested peatlands in eastern Canada. Ecosystems.

691   https://doi.org/10.1007/s10021-020-00483-x

692   Magnan G, Le Stum-Boivin É, Garneau M, Grondin P, Fenton N, Bergeron Y (2019) Holocene

693   vegetation dynamics and hydrological variability in forested peatlands of the Clay Belt, eastern

694   Canada, reconstructed using a palaeoecological approach. Boreas 48:131-146.

695   Magnan G, van Bellen S, Davies L, Froese D, Garneau M, Mullan-Boudreau G, …Shotyk S (2018)

696   Impact of the Little Ice Age cooling and 20th century climate change on peatland vegetation

697   dynamics in central and northern Alberta using a multi-proxy approach and high-resolution peat

698   chronologies. Quat Sci Rev 185:230-243.

699   Manzoni S, Čapek P, Porada P, Thurner M, Winterdahl M, Beer C, … Way D (2018) Reviews and

700   syntheses: Carbon use efficiency from organisms to ecosystems – definitions, theories, and

701   empirical evidence. Biogeosciences 15:5929-5949.

702   Marchand W, Gigardin MP, Hartmann H, Depardieu C, Isabel N, Gauthier S, … Bergeron Y (2020)

703   Strong overestimation of water-use efficiency responses to rising CO_2 in tree-ring studies. Glob

704   Change Biol. https://doi.org/10.1111/gcb.15166

705   Mauquoy D, Hughes PDM, van Geel B (2010) A protocol for plant macrofossil analysis of peat

706   deposits. Mires Peat 7:1-5.

707   Maynard DG, Paré D, Thiffault E, Lafleur B, Hogg KE, Kishchuk B (2014) How do natural

708   disturbances and human activities affect soils and tree nutrition and growth in the Canadian boreal

709   forest? Environ Rev 22:161-178.

710   McCarroll D, Loader NJ (2004) Stable isotopes in tree rings. Quat Sci Rev 23:771-801.

711   McKenney DW, Hutchinson MF, Papadopol P, Lawrence K, Pedlar J, Campbell K, … Owen T

712   (2011) Customized spatial climate models for North America. Bull Am Meteorol Soc December

713   1612-1622.

714   Naulier N, Savard MM, Bégin C, Marion J, Arseneault D, Bégin Y (2014) Carbon and oxygen

715   isotopes of lakeshore black spruce trees in northeastern Canada as proxies for climatic

716   reconstruction. Chem Geol 374-375:7-43.

717   Nicoll BC, Gardiner BA, Rayner B, Peace AJ (2006) Anchorage of coniferous trees in relation to

718   species, soil type, and rooting depth. Can J For Res 36:1871-1883.

719   O'Leary MH (1981) Carbon isotope fractionation in plants. Phytochemistry 20:553-567.

720   Pappas C, Maillet J, Rakowski S, Baltzer JL, Barr AG, Black TA, ... Sonnentag O (2020)

721   Aboveground tree growth is a minor and decoupled fraction of boreal forest carbon input. Agric

722   For Meteorol 290:108030.

723   Payette S (2001) Les principaux types de tourbières. In S Payette et L Rochefort (Eds.) Écologie

724   des tourbières du Québec-Labrador. Les Presses de l'Université Laval, Québec.

725   Payne RJ, Mitchell EAD (2009) How many is enough? Determining optimal count totals for

726   ecological and palaeoecological studies of testate amoebae. J Paleolimnol 42:483-495.

727   Peñuelas J, Canadell JG, Ogaya R (2011) Increased water-use efficiency during the 20th century

728   did not translate into enhanced tree growth. Glob Ecol Biogeogr 20:597-608.

729   Prescott CE, Maynard DG, Laiho R (2000) Humus in northern forests: friend or foe? For Ecol

730   Manag 133:23-36.

731   Primeau P, Garneau M. (under review). Carbon accumulation in peatlands following a boreal to

732   subarctic gradient in eastern Canada.

733   Puchi P, Castagneri D, Rossi S, Carrer M (2020) Wood anatomical traits in black spruce reveal

734   latent water constraints on the boreal forest. Glob Change Biol 26:1767-1777.

735   Pugh TAM, Müller C, Arneth A, Haverd V, Smith B (2016) Key knowledge and data gaps in

736   modelling the influence of CO2 concentration on the terrestrial carbon sink. J Plant Physiol 203:3-

737   15.

738   Reimer PJ, Bard E, Bayliss A, Beck JW, Blackwell PG, Bronk Ramsey C, … van der Plicht J

739   (2013) IntCal13 and MARINE13 radiocarbon age calibration curves 0-50000 years calBP.

740   Radiocarbon 55:1869-1887.

741   Robitaille M, Garneau M, van Bellan S. (submitted).

742   Rocha AV, Goulden ML, Dunn AL, Wofsy SC (2006) On linking interannual tree ring variability

743   with observations of whole-forest CO_2 flux. Glob Change Biol 12:1378-1389.

744   Ruppel M, Väliranta M, Virtanen T, Korhola A (2013) Postglacial spatiotemporal peatland

745   initiation and lateral expansion dynamics in North America and northern Europe. Holocene

746   23:1596-1606.

747   Saucier J-P, Robitaille A, Grondin P (2009) Cadre bioclimatique du Québec. In R Doucet, M Côté

748   (Eds.) Manuel de foresterie, 2nd edn. Éditions MultiMondes, Québec.

749   Saurer M, Cherubini P, Bonani G, Siegwolf R (2003) Tracing carbon uptake from a natural CO2

750   spring into tree rings: an isotope approach. Tree Physiol 23:997-1004.

751   Saurer M, Spahni R, Frank DC, Joos F, Leuenberger M, Loader NJ, … Young GHF (2014) Spatial

752   variability and temporal trends in water-use efficiency of European forests. Glob Change Biol

753   20:3700-3712.

754   Scheidegger Y, Saurer M, Bahn M, Siegwolf R (2000) Linking stable oxygen and carbon isotopes

755   with stomatal conductance and photosynthetic capacity: a conceptual model. Oecologia 125:350-

756   357.

757   Schneider L, Esper J, Timonen M, Büntgen U (2014) Detection and evaluation of an early

758   divergence problem in northern Fennoscandian tree-ring data. Oikos 123:559-566.

759   SCIEM (2019) PAST5: Personal Analysis System for Tree Ring Research version 5.0.610. SCIEM,

760   Viennes.

761   Silva LCR, Horwath WR (2013) Explaining Global Increases in Water Use Efficiency: Why Have

762   We Overestimated Responses to Rising Atmospheric CO2 in Natural Forest Ecosystems? PloS one

763   8:e53089 (5p).

764   Simard M, Lecomte N, Bergeron Y, Bernier PY, Paré D (2007) Forest productivity decline caused

765   by successional paludification of boreal soils. Ecol Appl 17:1619-1637.

766   Simard M, Bernier PY, Bergeron Y, Paré D, Guérine L (2009) Paludification dynamics in the boreal

767   forest of the James Bay Lowlands: effect of time since fire and topography. Can J For Res

768   33:546-552.

769   Skomarkova MV, Vaganov EA, Mund M, Knohl A, Linke P, Boerner A, Schulze E-D (2006) Inter-

770   annual and seasonal variability of radial growth, wood density and carbon isotope ratios in tree

771   rings of beech (*Fagus sylvatica*) growing in Germany and Italy. Trees 20:571-586.

Szeicz JM, MacDonald GM (1994) Age-dependent tree-ring growth responses of subarctic white spruce to climate. Can J For Res 24:120-132.

Tamm CO (1991) Nitrogen in terrestrial ecosystems: questions of productivity, vegetational changes, and ecosystem stability. Springer-Verlag, Heidelberg.

Thompson DK, Simpson BN, Beaudoin A (2016) Using forest structure to predict the distribution of treed boreal peatlands in Canada. For Ecol Manag 372:19-27.

Tognetti T, Cherubini P, Innes JL (2000) Comparative stem-growth rates of Mediterranean trees under background and naturally enhanced ambient CO_2 concentrations. New Phytol 146:59-74.

Ung CH, Bernier P, Guo XJ (2008) Canadian national biomass equations: new parameter estimates that include British Columbia data. *Can J For Res* 38:1123–1132.

van Bellen S, Magnan G, Davies L, Froese D, Mullan-Boudreau G, Zaccone C, … Shotyk W (2018) Testate amoeba records indicate regional 20th-century lowering of water tables in ombrotrophic peatlands in central-northern Alberta, Canada. Glob Change Biol 24:2758-2774.

Van Cleve K, Dyrness CT, Viereck LA, Fox J, Chapin FS, Oechel W (1983) Taiga ecosystems in interior Alaska. BioScience 33:39-44.

Van Cleve K, Viereck LA (1981) Forest succession in relation to nutrient cycling in the boreal forest of Alaska. In DC West, HH Shugart, DB Botkin (Eds.) Forest succession: concepts and application. Springer-Verlag, New-York.

van der Sleen P, Groenendijk P, Vlam M, Anten NPR, Boom A, Bongers F, … Zuidema PA (2015) No growth stimulation of tropical trees by 150 years of CO_2 fertilization but water-use efficiency increased. Nat Geosci 8:24-28.

793   Vicca S, Luyssaert S, Peñuelas J, Campioli M, Chapin FS, Ciais P, … Janssens IA (2012) Fertile

794   forests produce biomass more efficiently. Ecol Lett 15:520-526.

795   Viereck LA, Johnston WF (1990) *Picea mariana* (Mill.) B.S.P. In RM Burns & BH Honkala (Eds.)

796   Silvics of North America: 1. Conifers. US Department of Agriculture. Forest Service, Washington.

797   Vincent J-S, Hardy L (1977) L'évolution et l'extension des lacs glaciaires Barlow et Ojibway en

798   territoire québécois. Géo Phy Quat 31:357-372.

799   Vitousek PM, Howarth RW (1991) Nitrogen limitation on land and in the sea: how can it occur?

800   Biogeochemistry 13:87-115.

801   Walker X, Johnstone JF (2014) Widespread negative correlations between black spruce growth and

802   temperature across topographic moisture gradients in the boreal forest. Environ Res Lett 9:064016

803   (9p).

804   Wang W, Liu X, An W, Xu G, Zeng X (2012) Increased intrinsic water-use efficiency during a

805   period with persistent decreased tree radial growth in northwestern China: Causes and implications.

806   For Ecol Manag 275:14-22.

807   Waterhouse JS, Switsur VR, Barker AC, Carter AHC, Hemming DL, Loader NJ, Robertson I

808   (2004) Northern European trees show a progressively diminishing response to increasing

809   atmospheric carbon dioxide concentrations. Quat Sci Rev 23:803-810.

810   Webster K, Bhatti JS, Thompson DK, Nelson SA, Shaw CH, Bona KA, … Kurz WA (2018)

811   Spatially-integrated estimates of net ecosystem exchange and methane fuxes from Canadian

812   peatlands. Carbon Balance Manag 13:1-21.

813   Wu G, Liu X, Chen T, Xu G, Wang W, Zeng X, Zhang X (2015) Elevation-dependent variations

814   of tree growth and intrinsic water-use efficiency in Schrenk spruce (*Picea schrenkiana*) in the

815   western Tianshan Mountains, China. Front Ecol Evol 6:309.

816   Yakir D (1992) Variations in the natural abundance of oxygen-18 and deuterium in plant

817   carbohydrates. Plant Cell Environ 15:1005-1020.